Food Research International 190 (2024) 114658

Contents lists available at ScienceDirect

Food Research International

journal homepage: www.elsevier.com/locate/foodres

Changes of structure properties and potential allergenicity of ovalbumin under high hydrostatic pressures

Jing Yang [a,b,*], Hong Kuang [a], Nandan Kumar [c], Jiajia Song [d], Yonghui Li [c,**]

[a] Chongqing Engineering Research Center for Processing & Storage of Distinct Agricultural Products, Chongqing Technology and Business University, Chongqing 400067, China
[b] School of Food Nutrition and Health (Hot Pot) Modern Industry, Chongqing Technology and Business University, Chongqing 400067, China
[c] Department of Grain Science and Industry, Kansas State University, Manhattan, KS 66506, USA
[d] College of Food Science, Southwest University, Chongqing 400715, China

ARTICLE INFO

Keywords:
High hydrostatic pressure
Ovalbumin
Structure property
IgE binding capacity
Combinational study

ABSTRACT

Egg proteins, notably ovalbumin (OVA), contribute to a prevalent form of food allergy, particularly in children. This study aims to investigate the impact of high hydrostatic pressure (HHP) treatment at varying levels (300, 400, 500, and 600 MPa) on the molecular structure and allergenicity of OVA. The structure of HHP-treated OVA was assessed through fluorescence spectroscopy, circular dichroism spectroscopy, and molecular dynamics (MD) simulation. HHP treatment (600 MPa) altered OVA structures, such as α-helix content decreased from 28.07 % to 19.47 %, and exogenous fluorescence intensity increased by 8.8 times compared to that of the native OVA. The free sulfhydryl groups and zeta potential value were also increased with HHP treatment (600 MPa). ELISA analysis and MD simulation unveiled a noteworthy reduction in the allergenicity of OVA when subjected to 600 MPa for 10 min. Overall, this study suggests that the conformational changes in HHP-treated OVA contribute to its altered allergenicity.

1. Introduction

In recent years, food allergies have emerged as a significant threat to human health, with a notable global increase in their incidence, imposing a considerable burden on both health and socio-economic aspects (Brough et al., 2020). Among young children, eggs and milk are the most crucial food allergens (Taniguchi, Ogura, Sato, Ebisawa, & Yanagida, 2022; Zhu, Vanga, Wang, & Raghavan, 2018). Egg white protein stands out as a widespread cause of food allergies globally, with a reported prevalence ranging from 1.6 % to 10.1 % (Taniguchi et al., 2022). Currently, the sole method to avoid egg allergy is abstaining from consuming food products containing egg white protein. Nevertheless, this is challenging due to the prevalence of processed foods containing egg-derived ingredients. Consequently, reducing the allergenic potential of egg white protein is essential to mitigate its associated risks. Several studies have indicated that certain food processing technologies, such as conventional thermal treatment, can decrease allergenicity by modifying the structures of egg white protein (W. H. Yang, Tu, Wang, Li, & Tian, 2017; Zhang et al., 2018; Zhu et al., 2018). However, these treatments can cause alterations in flavor and nutrient composition of egg whites, thereby impacting product quality and consumer preferences (Abeyrathne, Lee, & Ahn, 2013; Zhu et al., 2018). Due to the inherent resistance of food allergens to thermal treatment and protein enzymes, commonly employed traditional food processing methods often fail to eliminate their potential allergenicity (López-Expósito et al., 2008). Consequently, there has been a recent exploration of innovative non-thermal methods to address these challenges.

High hydrostatic pressure (HHP), utilized as a non-thermal processing technology, achieves sterilization and enzyme inactivation at room temperature. This approach is employed to maintain the freshness and nutritional integrity of various food products (Hogan, Kelly, & Sun, 2005). Several reviews have pointed out that HHP has the potential to modify the allergenicity of various proteins, attributed to structural changes. These changes can result in processes such as aggregation, fragmentation, denaturation, or gelatinization (Jiang et al., 2023; Pan et al., 2019; Yu et al., 2023). The application of HHP treatment leads to notable alterations in the composition of egg white proteins, affecting aspects such as size, microstructure, and secondary structure (Z. Zhang

* Corresponding author at: Chongqing Technology and Business University, Chongqing 400067, China.
** Corresponding author at: Kansas State University, Manhattan, KS 66506, USA.
E-mail addresses: jyang@ctbu.edu.cn (J. Yang), yonghui@ksu.edu (Y. Li).

https://doi.org/10.1016/j.foodres.2024.114658
Received 5 March 2024; Received in revised form 15 June 2024; Accepted 15 June 2024
Available online 16 June 2024

et al., 2020). Reports indicate that the structural changes during HHP reduce antigenicity or allergenicity of allergens in whey proteins (Jiang et al., 2023; Meng, Bai, Gao, Li, & Chen, 2017). Consequently, HHP treatment holds promise for diminishing the allergenicity of egg white protein. Studies have shown that IgE-binding ability of egg white allergens is reduced by the combined application of HHP (400–700 MPa, 20 min) and heat (70 °C), accompanied by alterations in protein structure (Hildebrandt et al., 2010). Ovalbumin (OVA) stands out as a primary allergen within egg white protein (W. Yang, Tu, Wang, Zhang, & Song, 2018). However, the structure changes and immunoreactivity of OVA during HHP processing treatment remain unclear.

The influence of HHP treatment on both the allergenicity and structural changes of OVA was investigated in this study. Additionally, it aims to elucidate the potential mechanisms behind alterations in immunoreactivity resulting from structural modifications induced by HPP. Circular dichroism (CD) spectroscopy, fluorescence spectroscopy, and SDS-PAGE were employed to analyze secondary and tertiary structures. The binding of immunoglobulin E (IgE) to OVA was assessed using enzyme-linked immunosorbent assay (ELISA). All these experimental methods were combined with molecular dynamics (MD) simulation to understand the changes in the allergenicity of OVA. The findings of this study offer essential insights into HPP-reduced allergenicity of OVA, contributing valuable information to the understanding of these processes.

2. Materials and methods

2.1. Reagents and materials

OVA (A5503) and 1-anilinonaphthalene-8-sulfonate (ANS, A1028) were purchased from Sigma-Aldrich (St. Louis, MO, USA). Goat anti-Mouse IgE Secondary Antibody (SA5-10262), HRP (SA5-10263) and Imject^{TM} Alum (77161) were obtained from Thermo Fisher Scientific (Shanghai, China). SDS-PAGE sample loading buffer 2 × (P0015B) , Coomassie Brilliant Blue R-250 (P0017B), Tetramethylbenzidine (TMB, P0215), and protein molecular weight marker (P0060S) were obtained from Beyotime Biotechnology (Shanghai, China). All other reagents and chemicals were of analytical grade.

2.2. Preparation of OVA specific polyclonal antibodies

Three-week-old female BALB/c mice were procured from Hunan Silaikejingda Experimental Animal Co. in China. All animal experimental procedures were approved by the Animal Ethics Committee of Southwest University (Chongqing, China, NO.20231229–01). The mice were housed in an environment with 12-hour light/dark cycle at 25 ± 1 °C, and free access to water and food. Following a one-week acclimatization period, 30 mice were divided into two groups (Fig. S1): a control group (n = 10 mice) and an OVA-induced allergy group (n = 20 mice). On days 0, 7, 14, and 21, mice in the allergy group were intraperitoneally (i.p.) injected with 50 μg of OVA dissolved in 150 μL PBS and 50 μL alum adjuvant, while the control group received injections of 200 μL PBS/alum adjuvant mixture without OVA. Subsequently, mice in in the allergy group were orally gavage with 50 μg of OVA dissolved in 200 μL PBS on days 28, 31, 34, 37, 40, 43, 46. On day 49, a final challenge was administered through oral gavage with 20 mg of OVA dissolved in 200 μL PBS (Y. Liu et al., 2021; Luo, Gan, Yu, Wu, & Xu, 2020). Allergic behaviors were observed in the mice within 1 h, and mice were quickly euthanized by cervical dislocation. The blood was then collected and centrifuged at 3000 × g, 4 °C for 10 min. The serum with high level of OVA-specific IgE (Fig. S2) was stored at −80 °C for IgE-binding ability analysis.

2.3. HHP treatments

OVA solution (1 mg/mL) was prepared with deionized water and packed into a special polyethylene bag (BZD085, Blueberry, Shanghai, China) and sealed. The samples were treated at 300 MPa, 400 MPa, 500 MPa, or 600 MPa for 10 min at 25 °C by a high-pressure apparatus (SHPP-2L, Shanxi, China). After HHP treatments, samples were transferred into a −80 °C freezer immediately, and then freeze-dried for further analysis.

2.4. IgE-binding ability analysis by indirect enzyme-linked immunosorbent assay (iELISA)

OVA IgE-binding ability was analyzed with the previous method from Zhao et al. (2022). Initially, OVA, either in its native form or treated with HHP, was dissolved in carbonate buffer (pH 9.6, 50 mmol/L). The resulting solution was added to 96-well microplates 4 °C overnight. Subsequently, the plates underwent three washes with phosphate-buffered saline containing 0.05 % Tween 20 (PBST) and were gently patted dry. Then, they were incubated with 5 % skimmed milk in PBST at 37 °C for 1 h. Following three washes with PBST, 50 μL of OVA-allergic mouse serum (1:100 in PBST) was applied and incubated at 37 °C for 1 h. Each well underwent immediate aspiration, followed by 5 washes with PBST, then incubated with IgE-HRP (1:2,000 in PBST) at 37 °C for 30 min. After another 5 washes with PBST, TMB was added and incubated at 37 °C for 15 min, which was halted by sulfuric acid (2 mol/L), and the optical density (OD) is measured at 450 nm using a microplate reader (Infinite M200 Pro, Tecan, Männedorf, Switzerland).

2.5. Analysis of protein molecular weight by sodium dodecyl sulfate–polyacrylamide gel electrophoresis (SDS-PAGE)

OVA molecular weight changes were analyzed following the previous method (Lu et al., 2018). A 12 % separating gel and 5 % concentrate gel were prepared. OVA solution (1 mg/mL) was heated and centrifuged, then mixed with 1 × loading buffer in a sample loading volume. Electrophoresis was performed, and the gel was stained with Coomassie Brilliant Blue R-250.

2.6. Scanning electron microscope (SEM) analysis

The OVA samples were uniformly coated on a silicon wafer and adhered to a metal platform with conductive adhesive. A conductive gold layer was sputter-plated (M. Li, Li, Tan, Liu, & Duan, 2019). The morphology of the OVA was observed using SEM (SU-3500, Hitachi, Tokyo, Japan) at 50 and 500 × magnifications.

2.7. Circular dichroism (CD) analysis

The secondary structure changes of OVA after HHP treatment were assessed by CD spectroscopy. The OVA samples (0.2 mg/mL) were scanned using CD spectroscopy (Chirascan, Applied Photophysics, Surrey, UK). All CD experiments were carried out at 25 °C, with a bandwidth of 1.0 nm. The results were expressed as ellipticity in millidegrees (mdeg). Content analysis of various secondary structures in OVA were obtained by combining deep neural networks (CDNN) (W. Yang et al., 2018).

2.8. Intrinsic fluorescence spectrum analysis

Intrinsic fluorescence spectra were measured with a fluorescence spectrometer (F-7000, Hitachi, Tokyo, Japan). Excitation of protein fluorescence occurred at 280 nm, and emission spectra were captured within the range of 310–400 nm. The intrinsic fluorescence characteristics of HHP-treated OVA were examined at a protein concentration of 0.1 mg/mL (Y. Li et al., 2022).

2.9. Exogenous fluorescence spectrum analysis

ANS (4 mmol/L) in PBS (10 mmol/L, pH 7.0) was mixed with OVA solution (0.1 mg/mL) at a ratio of 1: 50 (v/v). The exogenous fluorescence profile of HHP-treated OVA was tested by fluorescence spectrometer (F-7000, Hitachi, Tokyo, Japan), with the excitation wavelength (390 nm) and the emission spectra (410–600 nm) (W. Yang et al., 2018).

2.10. Free sulfhydryl (SH) analysis

The content of free SH groups in OVA after HHP treatment was determined according to the previous method (M. Li et al., 2019). OVA (1 mg/mL) was prepared using Tris-glycine buffer (86 mmol/L Tris, 4 mmol/L EDTA-Na, 90 mmol/L Glycine, pH 8.0). Ellman's reagent (DTNB dissolved in Tris-glycine buffer at a concentration of 4 mg/mL) was mixed with the protein solution at a ratio of 1:100 (v/v). After incubating in the dark at 25 °C for 1 h, the OD is measured at 412 nm using a spectrophotometer (UV-1102, Tianmei Techcomp, Shanghai, China). Calculation of free sulfhydryl content: SH (μ mol/g) = 73.53 × A_{412}/C, where A_{412} is the absorbance of the sample at 412 nm and C represents the sample concentration.

2.11. Zeta potential analysis

The OVA samples with different treatments were dissolved in PBS solution (10 mmol/L, pH 7.0) at 1 mg/mL. The zeta potential of protein solution was determined using a zeta potential analyzer (ZEV3600, Malvern Instruments, Worcestershire, UK) (M. Li et al., 2019).

2.12. Molecular dynamics simulation

The 3D structure of OVA (UniProt ID: A0A2H4Y8A9) was sourced from AlphaFold's AF-A0A2H4Y8A9-F1 prediction within the AlphaFoldDB 3D structure database (David, Islam, Tankhilevich, & Sternberg, 2022). The GROMACS software (Abraham et al., 2015), version 2023.3, was used to run a comprehensive molecular dynamics (MD) simulation with CHARMM force field (Bjelkmar, Larsson, Cuendet, Hess, & Lindahl, 2010), while the protein was solvated within an TIP3P water model. The system was neutralized by adding counter ions, *i.e.,* 11Na^+ ions into the solvated box. Then the system was subjected to a rigorous minimization, including 2000 steps of steepest descent followed by 5000 steps of conjugate-gradient minimizations, ensuring efficient relaxation and convergence to a stable energy state (Kumar, Sarma, & Sastry, 2022; Kumar & Sastry, 2021). The system was then equilibrated for 500 ps and 1000 ps under NVT and NPT conditions, respectively. Finally, production run was conducted for a cumulative duration of 2.5 μs, with individual simulations lasting 500 ns each, followed by an integration time step of 0.2 ps. All bonds in the system were constrained by LINCS algorithm. The V-rescale thermostat facilitated weak coupling to an external bath, preserving the system at a constant temperature of 298.15 K. Trajectory coordinates were recorded at 2 ps intervals throughout the simulation. Pressure coupling was executed utilizing the isotropic Parrinello-Rahman protocol, sequentially targeting pressures of 0.1 (control), 300, 400, 500, and 600 MPa, respectively.

2.13. Statistical analysis

All images were plotted and modified using GraphPad prism software 9 (GraphPad Software Inc., San Diego, CA, USA). All data were tested for significance applying ANOVA (one-way) and Duncan's multiple range test under the significance level of $p < 0.05$ in SPSS statistics 23 (IBM Inc., Chicago, IL, USA).

3. Results

3.1. Effects of HHP on the microstructure and molecular weight of OVA

SEM was conducted to gain a better understanding of the microstructure of OVA treated by HHP. The surface of untreated OVA appears smooth and flaky (Fig. 1 A-B). HHP treatment disrupted the initially dense and smooth state of OVA, causing varying degrees of surface cracking. In the 400 MPa and 500 MPa treatment groups, some structures still resemble untreated OVA. However, the 600 MPa treatment group exhibited the highest level of fragmentation, revealing more small fragments compared to the other treatment groups.

SDS-PAGE analysis was conducted to elucidate the influence of HHP treatment on the molecular weight of OVA. In Fig. 1C, it is observed that the molecular weight of untreated OVA is around 42 kDa, which is similar to its theoretical molecular weight of 42,869 Da in Uniprot database. After HHP treatment, the migration rate of OVA remains the same as untreated OVA, and no new bands of lower molecular weight were observed. These outcomes indicated that the peptide bonds in primary structure of OVA may not be affected by HHP treatments within the range of 300 MPa to 600 MPa.

3.2. Effects of HHP on the free SH groups and Zeta potential of OVA

Zeta potential is another crucial parameter for evaluating the aggregation state of proteins. Isoelectric point of OVA is 4.7, which carries a negative charge at a sample pH of 7.0 (H. Li, Zhu, Zhou, Peng, & Guo, 2016). As shown in Fig. 2A, HHP treatments (300 MPa to 500 MPa) significantly increased the Zeta potential of OVA indicating that HHP-treated OVA surfaces contain more negatively charged amino acids compared to untreated OVA. The larger the absolute value of the Zeta potential, the higher the electrostatic repulsion between proteins (Long, Fan, & Zhang, 2023). However, the Zeta potential decreased with further increased pressure to 600 MPa, though it remained 1.16 times that of the untreated group.

The level of free SH is closely associated with the dissociation of disulfide bonds, reflecting the exchange reaction between −SH and S-S. The creation of disulfide bonds and the inclusion of protein molecules in the aggregation process can result in a reduction in free thiol content, impacting the interaction of allergenic sites with IgE (Shriver & Yang, 2011). As illustrated in Fig. 2B, compared to untreated OVA, the free SH content was decreased significantly by 41.92 % at a pressure of 300 MPa. As the pressure continued to increase, the free SH content correlated positively with pressure, reaching 1.80 times that of untreated OVA at 500 MPa and 6.28 times at 600 MPa. This indicates that HHP disrupted intramolecular disulfide bonds in proteins, exposing free SH as the protein molecules unfolded.

3.3. Effects of HHP on the molecular structure changes of OVA

CD spectroscopy is a crucial technique for studying variations in the secondary structure of proteins. The CD spectrum intensity of OVA, as depicted in Fig. 3A, was influenced by HHP treatments, signifying shifts in the secondary structure content of the OVA samples. Quantitative analysis of α-helix, β-sheet, β-turn, and random coil content in OVA was conducted (Fig. 3B). The CD spectrum of OVA exhibits a positive peak around 192 nm and negative peaks near 208 nm and 220 nm, characteristic of the α-helix structure in proteins (W. Yang et al., 2018). In untreated OVA, the α-helix is 28.07 %, which was initially decreased by different HHP treatments with a significant reduction to 19.47 % at 600 MPa. In untreated OVA, β-sheet (22.27 %), β-turn (17.43 %), and random coil (32.23 %) were observed. After HHP treatment at 600 MPa, the content of β-sheet, β-turn, and random coil was changed to 21.26 %, 19.97 %, and 39.30 %.

Intrinsic fluorescence spectroscopy commonly involves the measurement of fluorescence emitted by tryptophan or tyrosine residues in

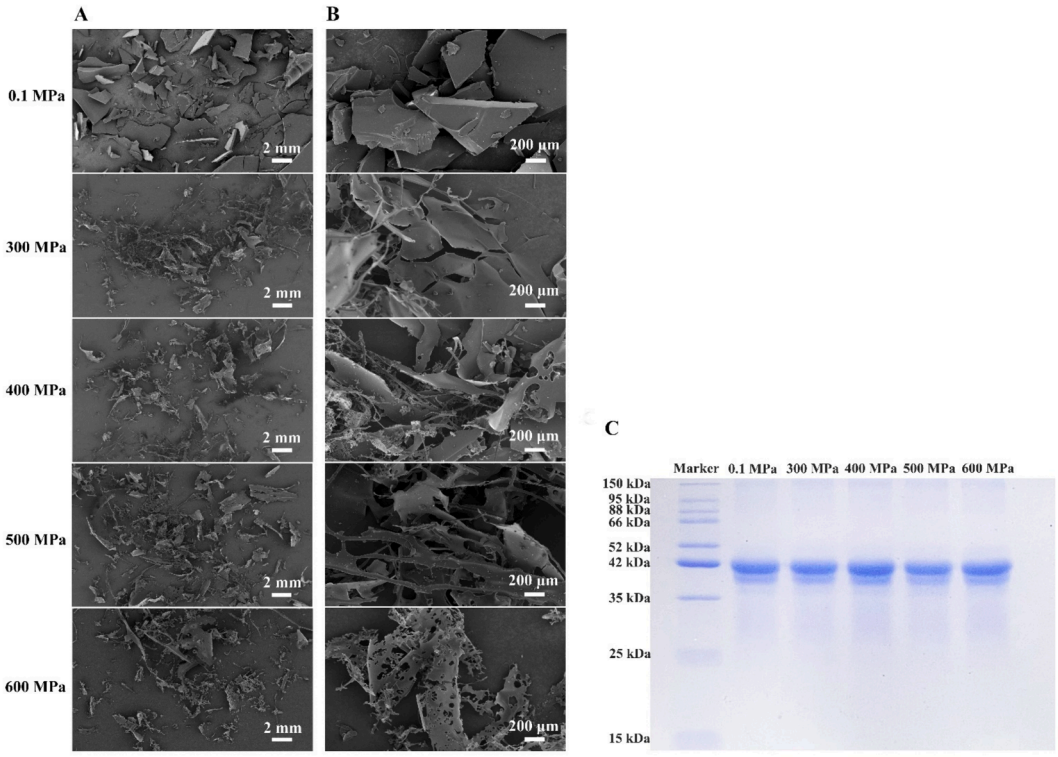

Fig. 1. Microstructure changes and molecular weight of OVA treated with high hydrostatic pressure. Morphology of OVA was determined by scanning electron microscopy. SEM images of OVA at 50 × magnification (A) and 500 × magnification (B); SDS-PAGE protein bands of OVA (C).

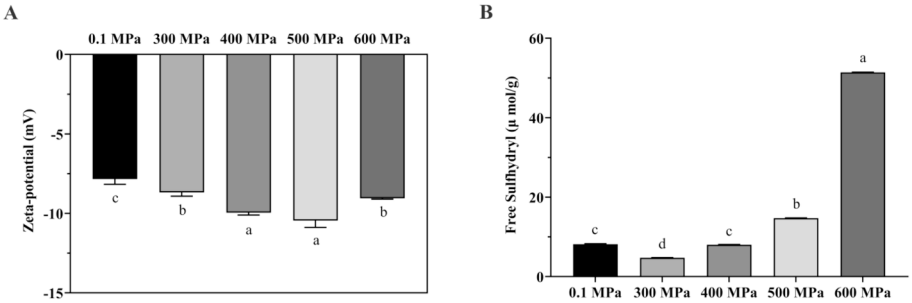

Fig. 2. Physical properties changes of OVA treated with high hydrostatic pressure. (A) Zeta potential; (B) Content of free surface sulfhydryl groups. Data are presented as the mean ± standard error of the mean (SEM), n = 3. Different superscript letters in the figure indicate significant differences ($p < 0.05$).

proteins. This method is widely recognized as a standard approach for assessing alterations in the tertiary structure of proteins that reflect changes in the polarity of tryptophan microenvironments (Y. Li et al., 2022). As shown in Fig. 3C, HHP treatments significantly reduced the fluorescence intensity of OVA compared to untreated OVA. This reduction was inversely associated to the treatment pressure, decreasing from 294.3 arbitrary units (a.u.) at 0.1 MPa to 150.1 a.u. at 600 MPa. Hydrophobic interactions play a crucial role in stabilizing the tertiary and quaternary structures of proteins, and ANS is commonly employed as a fluorescence probe to detect protein surface hydrophobicity (Zhou et al., 2016). As shown in Fig. 3D, compared to untreated OVA, the exogenous fluorescence intensity of OVA was increased across the range of 300–600 MPa treatments. Among them, the 600 MPa treatment group exhibited the highest fluorescence intensity, which is 8.8 times that of untreated OVA. The spectra show a blue shift (leftward movement), shifting from 494.8 nm for untreated OVA to 492.8 nm (300 MPa), 483.4 nm (400 MPa), 479.6 nm (500 MPa), and 472.4 nm (600 MPa). All these results suggest that 600 MPa treatment induced structural unfolding in OVA, exposing hydrophobic regions and leading to an increase in fluorescence intensity.

3.4. Structural changes of HHP-treated OVA revealed by MD simulation

To investigate localized alterations in the OVA protein, comprised of 386 amino acid residues, MD simulations were conducted at various pressures: 0.1, 300, 400, 500, and 600 MPa. OVA predominantly consist of twelve helices (H1 to H12) and ten strands (B1 to B10), as shown in Fig. 4A.

A total of 2.5 μs of MD simulations was conducted, with each individual simulation lasting 500 ns, to elucidate the conformational alterations in OVA protein. The changes were evaluated by superimposing the control structure (0.1 MPa) with those obtained after each pressure treatments (300–600 MPa). The simulation was employed to evaluate conformational changes (Fig. 4 B-E). In Fig. 5, the helical structure gradually diminished and the loop conformation near H7 helix (around Asp68-Val80) went through a significant fluctuation with increasing pressure. Additionally, the β-sheet was observed to be disrupted. For example, along with the transition of the loops/helices of Asp68-Val80,

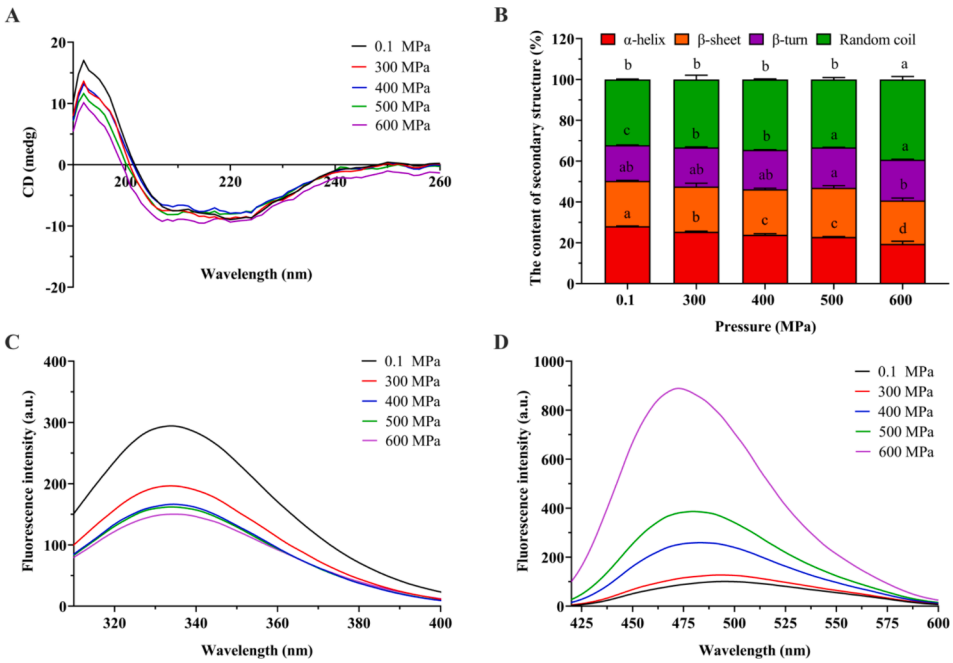

Fig. 3. Molecular structure changes of OVA treated with high hydrostatic pressure. (A) Circular dichroism spectra; (B) Secondary structure changes of OVA; (C) Intrinsic fluorescence spectra; (D) Exogenous fluorescence spectra. Data are presented as the mean ± standard error of the mean (SEM), n = 3. Different letters in Fig. 2 Fig. 3B indicate significant differences ($p < 0.05$).

Asp191-Asp193 and Val342-Ser354 to helices, a distinctive disruption was observed in one of the β-sheet (B1; Leu283 to Ser296) at 600 MPa, and B9 (Phe199-Lys207) appeared to be disappearing (except for 400 MPa), marking a significant deviation from the structural changes observed at lower pressures, such as the control at 0.1 MPa. Interestingly, the other β-sheet length (B2 to B4) appeared shorter and B5-B6 elongated slightly under higher pressures compared to the control, suggesting potential alterations. Notably, no evident disruption of B1 β-sheet was observed at the other pressures. These findings suggest a pressure-sensitive nature within specific β-sheets of the OVA protein, revealing their varying susceptibilities to pressure-induced conformational changes. The structural disruption of the protein caused by high pressure supports the findings obtained using CD spectroscopy (Fig. 2 Fig. 3A-B), which suggested structural alteration and unfolding at high pressures, especially at 600 MPa. Furthermore, the H7 helix and the loop connecting H7 and H3 exhibited conformational changes. Notably, the loop near the H7 helix appeared to transition from loop to helix, particularly at high pressures (Fig. 5C). These observations suggest that different regions of OVA are differentially affected by pressure treatment, resulting in varied changes in the secondary structure of their local regions. The disulfide bond between Cys74 and Cys121 was also affected by pressure. As shown in Fig. 5D, disulfide bond angle and dihedral changed significantly with increasing pressure, reflecting the changing conformation of residues Cys74.

Gyration analysis revealed an intriguing trend in the structural response of OVA protein to pressure. Under the control pressure (0.1 MPa), it exhibited a higher gyration, indicates a more expanded and relaxed state. However, as pressure increased significantly (300 to 600 MPa), a consistent decrease in gyration was observed (Fig. 6). This suggests a remarkable transition to a more compact and dense conformation. The observed structural alterations, such as the disappearance of helical structures and disruptions in β-sheets, likely contributed significantly to this compactness. At the highest pressure (600 MPa), OVA exhibited the lowest gyration, indicating a highly compressed and tightly packed state. This remarkable adaptation highlights OVA's inherent ability to undergo significant structural rearrangements to effectively accommodate extreme pressure environments.

3.5. Effect of HHP on the changes of IgE-binding capacity and IgE epitopes of OVA

The iELISA method was selected to examine how HHP treatments affect the IgE-binding ability of OVA. The serum containing OVA-specific IgE was collected from mice allergic to OVA (Fig. S1 and S2). The clinical symptoms of the allergic mice were investigated in both the control group and the allergy group. In the control group, the clinical score was less than 1, and the mice exhibited strong mobility and smooth, shiny fur after the final challenge. In contrast, the sensitized mice (allergy group) had clinical scores ranging from 2 to 5 and displayed symptoms such as loss of consciousness, no response to prodding, shortness of breath, shivering, and curled hair. Additionally, a high level of OVA-specific IgE was observed in the serum of the allergic mice compared to the control mice. These findings indicate that the OVA allergic model was successfully established, and the OVA-specific IgE in the serum was ready for use in the IgE-binding capacity assay.

As shown in Fig. 7A, the IgE-binding capacity of OVA initially increased and then decreased with varying pressure levels (300–600 MPa). Compared to untreated OVA, an increased IgE-binding ability was found when the pressure raised to 300 MPa. As the pressure continued to increase (400 MPa and 500 MPa), the IgE-binding capacity decreased. Upon further increasing the pressure to 600 MPa, the IgE-binding capacity decreased by 24.13 % reduction compared to untreated OVA. The IgE epitopes on OVA have been extensively characterized in the literature (Gazme, Rezaei, & Udenigwe, 2022). Understanding the conformational changes induced by high pressure on these epitopes helps to establish a correlation between structural alterations and the accessibility and exposure of specific IgE-binding sites. Fig. 7B revealed significant conformational changes in certain residues or patches of residues within epitopes (antigen-binding sites) (Gazme et al., 2022) of the OVA protein under high-pressure treatment. For instance, residues Tyr125 to Gly128 exhibit notable conformational changes, with the most pronounced alterations occurring at 300 MPa. Additionally, residues 188–200 and 141–176 also show significant conformational changes, including a partial loss of helix and β-sheet structures. These structural modifications at 300 MPa could expose more binding sites for

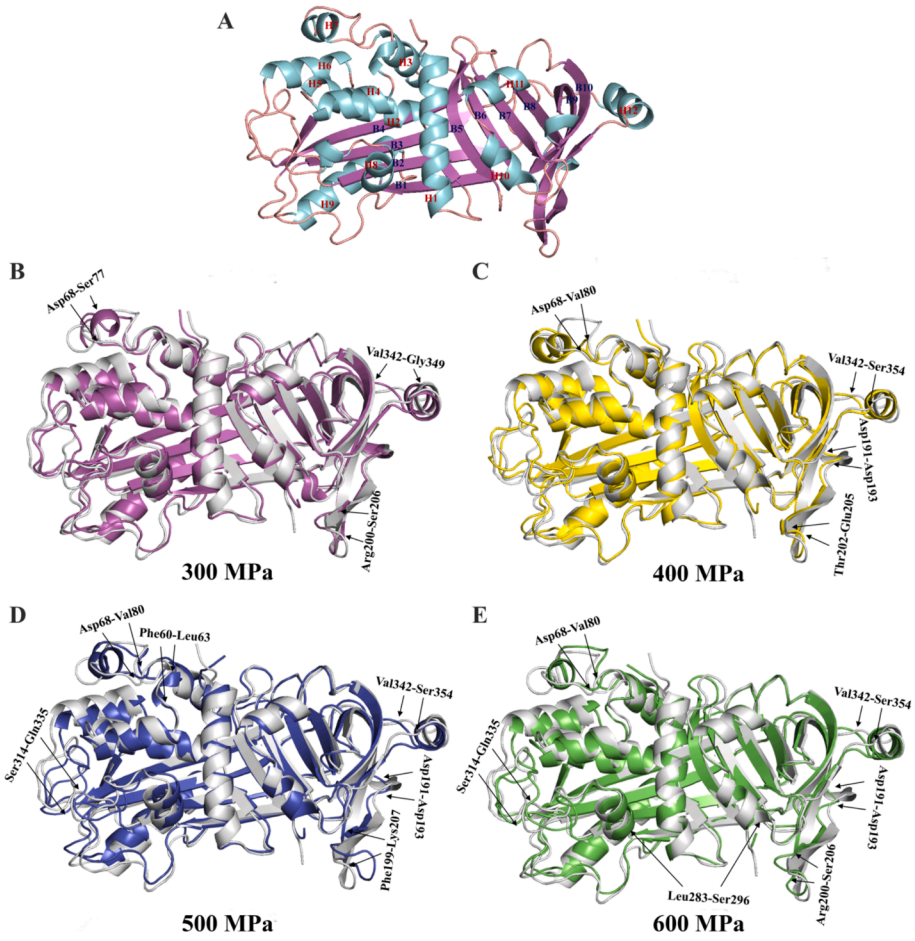

Fig. 4. The conformational analysis of OVA revealed through MD simulation. (A) The structure of OVA in its monomeric state, colored based on secondary structure, as follows: helix (light cyan; H1 to H12), beta sheet (light purple; B1 to B10), and loop (tints). (B-E) The conformational change of OVA under different high hydrostatic pressures. The structure colored by gray is the initial structure of OVA, and the structures colored magenta, yellow, blue, and green are the OVA structures obtained at 300, 400, 500, and 600 MPa, respectively.

IgE, potentially explaining the increased binding observed at this pressure. Overall, the MD simulations suggest that high hydrostatic pressure (HHP) treatments can alter the allergenicity of the OVA protein, offering valuable insights for further research in this field.

4. Discussion

HHP treatment effectively reduces the allergenicity of food allergens. The anomalous immune responses elicited by egg white protein, as observed in clinical studies, are predominantly attributed to IgE. Consequently, research on allergenicity has principally centered around food allergies mediated by IgE (H. Zhang et al., 2020). After high-pressure treatment, it was found that the IgE-binding capability of β-lactoglobulin (β-LG) was lowest at 200 MPa, while the highest binding capability was observed at 400 MPa (H. Zhang et al., 2020). The allergenicity of soy protein isolate (SPI) reduced by more than 50 % following HHP treatments (300, 400, 500 MPa, 20 min) (H. Li, Zhu, Zhou, & Peng, 2012). The IgE-binding ability of egg white allergens declined with rising pressure in both heat (70 °C) and HHP treatments (400–700 MPa, 20 min). These alterations in protein structure exhibited a positive correlation with pressure (Hildebrandt et al., 2010). In our study, we focused on the impact of HHP on the allergenicity of OVA and structural change. All the findings suggested that the HHP (600 MPa) potentially decreased the allergenicity of OVA with reduced IgE-binding ability and structural changes.

Several reviews have highlighted that HHP induces changes in the allergenicity of various proteins through structural modifications, resulting in processes such as aggregation, fragmentation, denaturation, or gelatinization. HHP has been considered to decrease the allergenicity of proteins through facilitating the unfolding of their secondary structure, without affecting the primary structure. HHP treatment does not disrupt these covalent bonds between protein molecules, thereby preserving protein's primary structure (Lv et al., 2022). SDS-PAGE is an important tool for evaluating protein molecular weight (Wang, Wang, Kranthi Vanga, & Raghavan, 2021). According our results of SDS-PAGE, the protein bands in OVA were not changed after HHP treatment compared to native OVA, indicating that HHP did not impact the primary structure of OVA. Similar findings have been reported in studies on other allergenic proteins subjected to HHP treatments. Protein bands of the peanut protein Ara h1 treated by different pressures (200–600 MPa) was similar with the native samples (Pan et al., 2019). Gluten protein in wheat was treated by HHP (200–500 MPa) for 5–25 min, and the molecular weight protein bands in the SDS-PAGE were same as the untreated gluten (Yao, Jia, Lu, & Li, 2022). β-LG was applied by pressure treatments (100–500 MPa for 30 min), and both the treatment and control groups produced bands of 18 kDa (Meng et al., 2017). Moreover, HHP has the potential to diminish the allergenicity of proteins by facilitating the unfolding of their secondary structure. The reduced α-helix content in Ara h1 under HHP treatments could induce the disruption of conformational epitopes, resulting in a reduced immunoreactivity of Ara h1 (Pan et al., 2019). In the case of Todp1 (TMTp1), a protein from squid muscle treated at 600 MPa, the conversion of α-helix

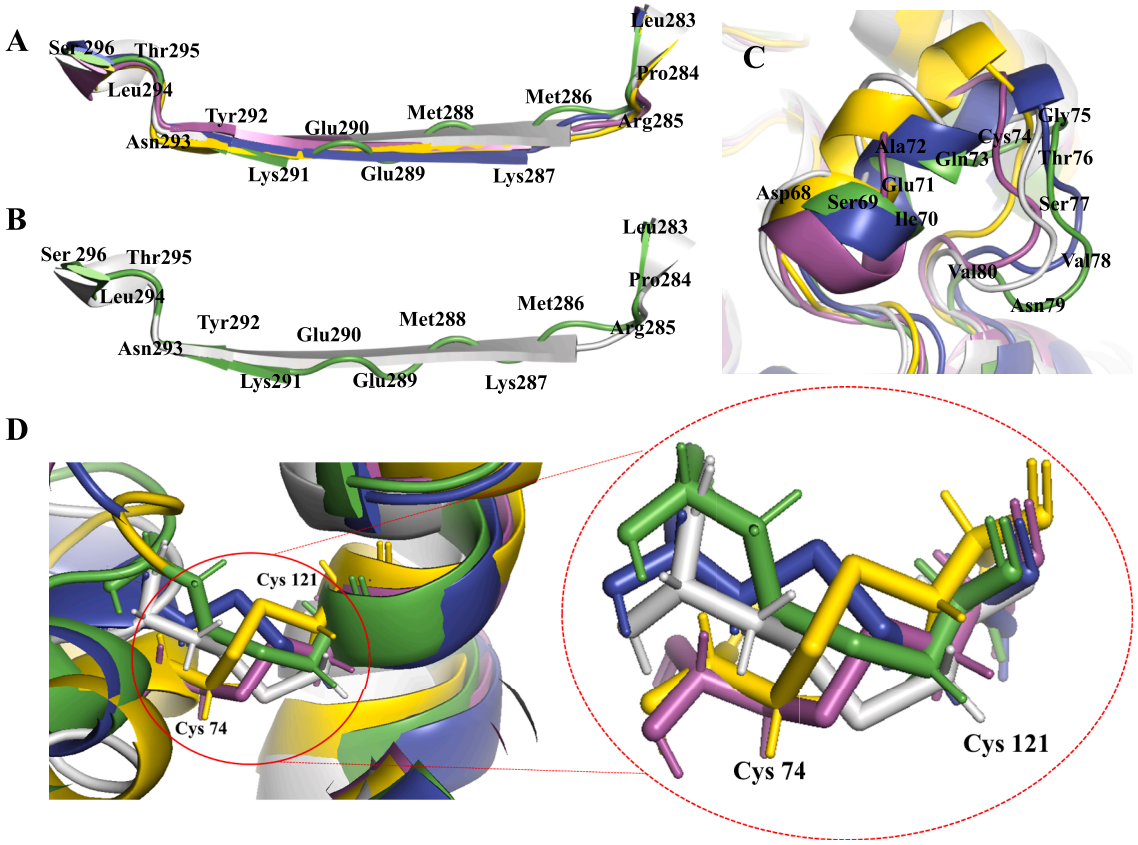

Fig. 5. Changes in the secondary structure and disulfide bonds of the local region of OVA treated with high hydrostatic pressure. (A) Superimposed B1 helix of the initial structure with B1 helices obtained at different pressures; (B) Superimposed B1 helix of the initial structure with B1 helix obtained at 600 MPa; (C) Superimposed H3 and H7 helices and loops between H3 and H7 helices of the initial structure and structures obtained at different pressures; (D) The disulfide bond between Cys74 and Cys121 of H7 and H6 of OVA at different pressures. The gray color represents the initial structure, while magenta, yellow, blue, and green represent the OVA structure obtained at 300, 400, 500, and 600 MPa, respectively.

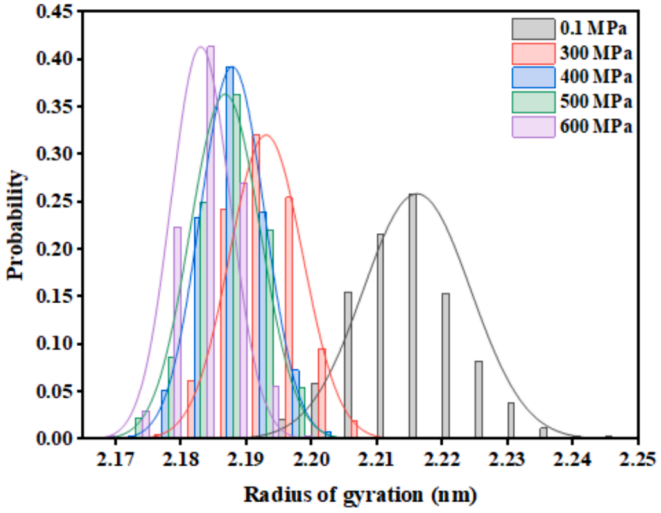

Fig. 6. Probability distribution of the radius of gyration for the OVA treated with high hydrostatic pressure.

to β-sheet and random coil resulted in allergenicity reduction (Jin et al., 2015). Similarly, α-helix content in soybean β-conglycinin was reduced by HHP, leading to a substantial decrease in allergenicity (Xi & He, 2018). These results indicate a close correlation between changes in α-helix structure content and allergenicity. In our study, α-helix content of OVA was more at 300 MPa than other pressures. Hydrogen bonds in proteins are the main force stabilizing secondary structures, and the α-helix structure is predominantly upheld by hydrogen bonds between carbonyl (−C = O) and amino (–NH2) groups within the peptide chain (Jiang et al., 2023; H. Zhang et al., 2020). HPP treatment can disrupt hydrogen bonds in proteins, potentially altering the stability of protein structures, including α-helix structures (Fanetti, Citroni, Dziubek, Nobrega, & Bini, 2018).

It is reported that the alterations in the tertiary structure of HHP-treated β-LG were more pronounced than those observed in the primary and secondary structures (Meng et al., 2017). Protein binds to conformation sensitive hydrophobic probe ANS and the changes of protein fluorescence indicating the surface hydrophobic characters and tertiary structure changes (Bhattacharjee & Das, 2000). A previous study also noted the reduction in intrinsic fluorescence and heightened binding of ANS to OVA following HHP treatment (Smith, Galazka, Wellner, & Sumner, 2000). In our study, the binding of ANS to OVA exhibited a significant increase following HHP treatment beyond 400 MPa. The heightened external fluorescence intensity suggested the unfolding of the protein, exposing numerous hydrophobic regions following HHP (Smith et al., 2000). Thus, the hydrophobicity of the HHP-treated OVA may increase. Besides, HHP treatment (600 MPa) significantly reduced the internal fluorescence intensity of OVA in our study. Tryptophan residues are typically concealed within the protein, and a decrease in tryptophan fluorescence intensity in protein may indicate its tertiary structural changes. The reduced fluorescence intensity may be attributed to protein structural unfolding, exposing tryptophan to the solvent, where it can be quenched by the environment (Z. Li et al., 2020). HHP (100–600 MPa) caused whey proteins unfolding with an increase in

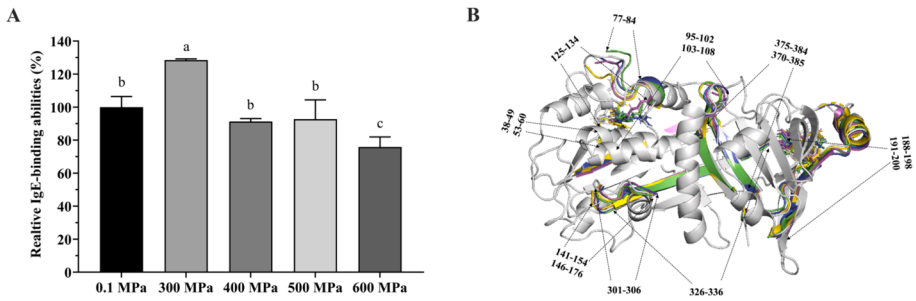

Fig. 7. Changes of IgE-binding capacities and IgE epitopes of OVA treated with high hydrostatic pressure. (A) IgE-binding abilities; (B) Initial structure of OVA is represented in gray, and the fluctuation of the local region (reported as epitopes (Gazme et al., 2022)) is illustrated in magenta (300 MPa), yellow (400 MPa), blue (500 MPa), and green (600 MPa). Data are presented as the mean ± standard error of the mean (SEM), n = 3. Different superscript letters in the figure indicate significant differences ($p < 0.05$).

surface hydrophobicity, which may due to the high pressure caused-dissociation and rearrangement of disulfide bonds, leading to the movement of free thiol groups from the interior of protein molecules to the external environment (Jiang et al., 2023; Yu et al., 2023). The exposed hydrophobic groups may then aggregate or recombine with each other, forming more stable structures (H. Li et al., 2012; Yao et al., 2022). Additionally, the blue shift in the fluorescence spectra suggests that HHP exposes certain non-polar groups, making the environment less polar (L. Liu, Li, Prakash, Dai, & Meng, 2018). As the environmental polarity decreases, the protein structure becomes looser (K. Liu et al., 2023).

Aggregation and conformational changes of OVA under HHP, which masked antigenic epitopes, may be related to its allergenicity. The IgE-binding ability of β-LG was decreased following treatment at pressures exceeding 300 MPa (Chen, Wu, Chen, Yang, & Yang, 2022). This decrease mainly due to changes of allergen structure, which hidden IgE-binding epitopes (Chen et al., 2022). Alterations in the antigenicity and potential allergenicity of β-LG and whey proteins treated with HHP were a result of protein unfolding. This unfolding process exposed hydrophobic groups and antigenic epitopes from internal regions of native molecule to the external surface (Jiang et al., 2023; Meng et al., 2017). HHP also reduces the allergenicity of tropomyosin Tod p1 (TMTp1) through a combination of unfolding and modification of secondary structure (Jin et al., 2015).

The allergenicity of proteins is associated with the integrity of allergenic sites, which include both linear and conformational epitopes. Specific antibodies (IgE) binding to these allergenic sites can trigger allergic reactions (W. H. Yang et al., 2017). Therefore, alterations in both linear and conformational epitopes can affect the binding between allergens and IgE (Zhou et al., 2016). The allergenicity of OVA is mainly related to its conformational epitopes (Meng et al., 2017). The IgE epitopes on OVA have been extensively characterized recently. The most frequent common sequences associated with the IgE binding activity of OVA are 326–332, 375–384, and 323–332 (Gazme et al., 2022). In Fig. 6, residues Tyr125 to Gly128 exhibit drastic conformational changes, with the most pronounced alterations observed at 300 MPa, followed by 400–600 MPa. Notably, these residues fall within reported IgE epitopes: residues 125–134 and 127–136 (Benede, Lopez-Exposito, Lopez-Fandino, & Molina, 2014; Yoshinori Mine & Yang, 2007). Furthermore, significant conformational changes are observed in the H7 helix and the loop between the H3 and H7 helices, particularly at higher pressures. This region encompasses the IgE epitopes formed by residues 77–84 (Yoshinori Mine & Yang, 2007). Residues 188–200 also exhibit significant fluctuations, with partial disappearance of helix and β-sheet structures. These residues (188–198 and 191–200) were identified as IgE epitopes. Beyond these regions, MD simulations indicate noticeable conformational changes in residues appearing after residue 300. Several IgE epitopes have been reported in these regions, including 236–336, 370–385 (Benede et al., 2014), 323–332, 375–384 (Y. Mine & Rupa, 2003), 323–339 (Janssen et al., 1999; Sun et al., 2010), and 347–385 (Gazme et al., 2022; Honma et al., 1996), These conformational changes generally accompany the transition to a more compact and dense protein conformation. These findings suggest that HPP treatments have the potential to change the allergenicity of the OVA protein.

5. Conclusion

This work described the structure and allergenicity changes of OVA observed under HHP treatments. The findings from both spectroscopic analysis and MD simulation suggested that the application of HHP had effects on both the tertiary structure and potential binding sites of OVA. Importantly, applying HHP at 600 MPa led to the alterations in the microstructure and unfolding of the molecular structure in OVA. These changes affected the status of IgE-binding epitopes within the protein, thereby potentially reducing the allergenicity of OVA.

CRediT authorship contribution statement

Jing Yang: Writing – review & editing, Supervision, Project administration, Funding acquisition, Conceptualization. **Hong Kuang:** Writing – original draft, Methodology, Investigation, Formal analysis, Data curation. **Nandan Kumar:** Writing – original draft, Software, Investigation. **Jiajia Song:** Writing – review & editing. **Yonghui Li:** Writing – review & editing, Supervision, Conceptualization.

Declaration of competing interest

The authors declare that they have no known competing financial interests or personal relationships that could have appeared to influence the work reported in this paper.

Data availability

The data that has been used is confidential.

Acknowledgements

This study was supported by Natural Science Foundation of Chongqing, China (Grant No. cstc2021jcyj-msxmX0712; cstc2021jcyj-msxmX0772), Science and Technology Research Program of Chongqing Municipal Education Commission, China (Grant No. KJQN202100802), Chongqing Special Project for Technological Innovation and Application Development, China (Grant No. CSTB2022TFII-OFX0016).

Appendix A. Supplementary material

Supplementary data to this article can be found online at https://doi.org/10.1016/j.foodres.2024.114658.

References

Abeyrathne, E. D., Lee, H. Y., & Ahn, D. U. (2013). Egg white proteins and their potential use in food processing or as nutraceutical and pharmaceutical agents–a review. *Poult Science, 92*(12), 3292–3299.

Abraham, M. J., Murtola, T., Schulz, R., Páll, S., Smith, J. C., Hess, B., & Lindahl, E. (2015). GROMACS: High performance molecular simulations through multi-level parallelism from laptops to supercomputers. *SoftwareX, 1*, 19–25.

Benede, S., Lopez-Exposito, I., Lopez-Fandino, R., & Molina, E. (2014). Identification of IgE-binding peptides in hen egg ovalbumin digested *in vitro* with human and simulated gastroduodenal fluids. *Journal of Agricultural Food Chemistry, 62*(1), 152–158.

Bhattacharjee, C., & Das, K. P. (2000). Thermal unfolding and refolding of β-lactoglobulin: An intrinsic and extrinsic fluorescence study. *European Journal of Biochemistry, 267*(13), 3957–3964.

Bjelkmar, P., Larsson, P., Cuendet, M. A., Hess, B., & Lindahl, E. (2010). Implementation of the CHARMM force field in GROMACS: Analysis of protein stability effects from correction maps, virtual interaction sites, and water models. *Journal of Chemical Theory and Computation, 6*(2), 459–466.

Brough, H. A., Nadeau, K. C., Sindher, S. B., Alkotob, S. S., Chan, S., Bahnson, H. T., Leung, D. Y. M., & Lack, G. (2020). Epicutaneous sensitization in the development of food allergy: What is the evidence and how can this be prevented? *Allergy, 75*(9), 2185–2205.

Chen, G., Wu, C., Chen, X., Yang, Z., & Yang, H. (2022). Studying the effects of high pressure–temperature treatment on the structure and immunoreactivity of β-lactoglobulin using experimental and computational methods. *Food Chemistry, 372*, Article 131226.

David, A., Islam, S., Tankhilevich, E., & Sternberg, M. J. (2022). The AlphaFold database of protein structures: A biologist's guide. *Journal of Molecular Biology, 434*(2), Article 167336.

Fanetti, S., Citroni, M., Dziubek, K., Nobrega, M. M., & Bini, R. (2018). The role of H-bond in the high-pressure chemistry of model molecules. *Journal of Physics: Condensed Matter, 30*(9), Article 094001.

Gazme, B., Rezaei, K., & Udenigwe, C. (2022). Epitope mapping and the effects of various factors on the immunoreactivity of main allergens in egg white. *Food & Function, 13*(1), 38–51.

Hildebrandt, S., Schütte, L., Stoyanov, S., Hammer, G., Steinhart, H., & Paschke, A. (2010). *In vitro* determination of the allergenic potential of egg white in processed meat. *Journal of allergy, 2010*, Article 238573.

Hogan, E., Kelly, A. L., & Sun, D.-W. (2005). High pressure processing of foods: An overview. *Emerging Technologies for Food Processing*, 3–24.

Honma, K., Kohno, Y., Saito, K., Shimojo, N., Horiuchi, T., Hayashi, H., Suzuki, N., Hosoya, T., Tsunoo, H., & Niimi, H. (1996). Allergenic epitopes of ovalbumin (OVA) in patients with hen's egg allergy: Inhibition of basophil histamine release by haptenic ovalbumin peptide. *Clinical & Experimental Immunology, 103*(3), 446–453.

Janssen, E. M., Wauben, M. H., Jonker, E. H., Hofman, G., Van Eden, W., Nijkamp, F. P., & Van Oosterhout, A. J. (1999). Opposite effects of immunotherapy with ovalbumin and the immunodominant T-cell epitope on airway eosinophilia and hyperresponsiveness in a murine model of allergic asthma. *American Journal of Respiratory Cell and Molecular Biology, 21*(1), 21–29.

Jiang, H., Zhang, Z., Wang, Y., Gao, J., Yuan, Q., & Mao, X. (2023). Effects of high hydrostatic pressure treatment on the antigenicity, structural and digestive properties of whey protein. *LWT, 178*, Article 114628.

Jin, Y., Deng, Y., Qian, B., Zhang, Y., Liu, Z., & Zhao, Y. (2015). Allergenic response to squid (*Todarodes pacificus*) tropomyosin Tod p1 structure modifications induced by high hydrostatic pressure. *Food and Chemical Toxicology, 76*, 86–93.

Kumar, N., Sarma, H., & Sastry, G. N. (2022). Repurposing of approved drug molecules for viral infectious diseases: A molecular modelling approach. *Journal of Biomolecular Structure and Dynamics, 40*(17), 8056–8072.

Kumar, N., & Sastry, G. N. (2021). Study of lipid heterogeneity on bilayer membranes using molecular dynamics simulations. *Journal of Molecular Graphics and Modelling, 108*, Article 108000.

Li, H., Zhu, K., Zhou, H., & Peng, W. (2012). Effects of high hydrostatic pressure treatment on allergenicity and structural properties of soybean protein isolate for infant formula. *Food Chemistry, 132*(2), 808–814.

Li, H., Zhu, K., Zhou, H., Peng, W., & Guo, X. (2016). Comparative study of four physical approaches about allergenicity of soybean protein isolate for infant formula. *Food and agricultural immunology, 27*(5), 604–623.

Li, M., Li, M., Tan, W., Liu, X., & Duan, X. (2019). Effects of ball-milling treatment on physicochemical and foaming activities of egg ovalbumin. *Journal of Food Engineering, 261*, 158–164.

Li, Y., Zhang, S., Ding, J., Zhong, L., Sun, N., & Lin, S. (2022). Evaluation of the structure-activity relationship between allergenicity and spatial conformation of ovalbumin treated by pulsed electric field. *Food Chemistry, 388*, Article 133018.

Li, Z., Kuang, H., Yang, J., Hu, J., Ding, B., Sun, W., & Luo, Y. (2020). Improving emulsion stability based on ovalbumin-carboxymethyl cellulose complexes with thermal treatment near ovalbumin isoelectric point. *Scientific Reports, 10*(1), 3456.

Liu, K., Lin, S., Liu, Y., Wang, S., Liu, Q., Sun, K., & Sun, N. (2023). Mechanism of the reduced allergenicity of shrimp (*Macrobrachium nipponense*) by combined thermal/pressure processing: Insight into variations in protein structure, gastrointestinal digestion and immunodominant linear epitopes. *Food Chemistry, 405*, Article 134829.

Liu, L., Li, Y., Prakash, S., Dai, X., & Meng, Y. (2018). Enzymolysis and glycosylation synergistic modified ovalbumin: Functional and structural characteristics. *International Journal of Food Properties, 21*(1), 395–406.

Liu, Y., Ma, Y., Chen, Z., Zou, C., Liu, W., Yang, L., Fu, L., Wang, Y., Liu, G.-M., & Cao, M.-J. (2021). Depolymerized sulfated galactans from Eucheuma serra ameliorate allergic response and intestinal flora in food allergic mouse model. *International Journal of Biological Macromolecules, 166*, 977–985.

Long, F. F., Fan, X. H., & Zhang, Q. A. (2023). Effects of ultrasound on the immunoreactivity of amandin, an allergen in apricot kernels during debitterizing. *Ultrasonics Sonochemistry, 95*, Article 106410.

López-Expósito, I., Chicón, R., Belloque, J., Recio, I., Alonso, E., & López-Fandiño, R. (2008). Changes in the ovalbumin proteolysis profile by high pressure and its effect on IgG and IgE binding. *Journal of Agricultural and Food Chemistry, 56*(24), 11809–11816.

Lu, Y., Li, S., Xu, H., Zhang, T., Lin, X., & Wu, X. (2018). Effect of covalent interaction with chlorogenic acid on the allergenic capacity of ovalbumin. *Journal of Agricultural and Food Chemistry, 66*(37), 9794–9800.

Luo, M., Gan, M., Yu, X., Wu, X., & Xu, F. (2020). Study on the regulatory effects and mechanisms of action of bifidobacterial exopolysaccharides on anaphylaxes in mice. *International Journal of Biological Macromolecules, 165*, 1447–1454.

Lv, X., Huang, X., Ma, B., Chen, Y., Batool, Z., Fu, X., & Jin, Y. (2022). Modification methods and applications of egg protein gel properties: A review. *Comprehensive Reviews in Food Science and Food Safety, 21*(3), 2233–2252.

Meng, X., Bai, Y., Gao, J., Li, X., & Chen, H. (2017). Effects of high hydrostatic pressure on the structure and potential allergenicity of the major allergen bovine β-lactoglobulin. *Food Chemistry, 219*, 290–296.

Mine, Y., & Rupa, P. (2003). Fine mapping and structural analysis of immunodominant IgE allergenic epitopes in chicken egg ovalbumin. *Protein Engineering, 16*(10), 747–752.

Mine, Y., & Yang, M. (2007). Epitope characterization of ovalbumin in BALB/c mice using different entry routes. *Biochimica et Biophysica Acta (BBA) - Proteins and Proteomics, 1774*(2), 200–212.

Pan, D., Tang, B., Liu, H., Li, Z., Ma, R., Peng, Y., Wu, X., Che, L., He, N., Ling, X., & Wang, Y. (2019). Effect of high hydrostatic pressure (HHP) processing on immunoreactivity and spatial structure of peanut major allergen Ara h 1. *Food and Bioprocess Technology, 13*(1), 132–144.

Shriver, S. K., & Yang, W. W. (2011). Thermal and nonthermal methods for food allergen control. *Food Engineering Reviews, 3*(1), 26–43.

Smith, D., Galazka, V. B., Wellner, N., & Sumner, I. G. (2000). High pressure unfolding of ovalbumin. *International Journal of Food Science & Technology, 35*(4), 361–370.

Sun, L. Z., Elsayed, S., Aasen, T., Van Do, T., Aardal, N., Florvaag, E., & Vaali, K. (2010). Comparison between ovalbumin and ovalbumin peptide 323–339 responses in allergic mice: Humoral and cellular aspects. *Scandinavian Journal of Immunology, 71*(5), 329–335.

Taniguchi, H., Ogura, K., Sato, S., Ebisawa, M., & Yanagida, N. (2022). Natural history of allergy to hen's egg: A prospective study in children aged 6 to 12 years. *International Archives of Allergy and Immunology, 183*(1), 14–24.

Wang, J., Wang, J., Kranthi Vanga, S., & Raghavan, V. (2021). Influence of high-intensity ultrasound on the IgE binding capacity of Act d 2 allergen, secondary structure, and In-vitro digestibility of kiwifruit proteins. *Ultrason Sonochemistry, 71*, Article 105409.

Xi, J., & He, M. (2018). High hydrostatic pressure (HHP) effects on antigenicity and structural properties of soybean β-conglycinin. *Journal of Food Science and Technology, 55*(2), 630–637.

Yang, W., Tu, Z., Wang, H., Zhang, L., & Song, Q. (2018). Glycation of ovalbumin after high-intensity ultrasound pretreatment: Effects on conformation, immunoglobulin (Ig)G/IgE binding ability and antioxidant activity. *Journal of the Science of Food and Agriculture, 98*(10), 3767–3773.

Yang, W. H., Tu, Z. C., Wang, H., Li, X., & Tian, M. (2017). High-intensity ultrasound enhances the immunoglobulin (Ig)G and IgE binding of ovalbumin. *Journal of the Science of Food and Agriculture, 97*(9), 2714–2720.

Yao, Y., Jia, Y., Lu, X., & Li, H. (2022). Release and conformational changes in allergenic proteins from wheat gluten induced by high hydrostatic pressure. *Food Chemistry, 368*, Article 130805.

Yu, X., Wang, X., Zhang, S., Zhang, Y., Zhang, H., & Yin, Y. (2023). Study on potential antigenicity and functional properties of whey protein treated by high hydrostatic pressure based on structural analysis. *Food Research International, 173*.

Zhang, H., Liao, H., Lu, Y., Hu, Y., Yang, H., Cao, S., & Qi, X. (2020). Effects of high hydrostatic pressure on the structural characteristics of parvalbumin of cultured large yellow croaker (*Larimichthys crocea*). *Journal of Food Processing and Preservation, 44*(12), e14911.

Zhang, Y., Wang, W., Zhou, R., Yang, J., Sheng, W., Guo, J., & Wang, S. (2018). Effects of heating, autoclaving and ultra-high pressure on the solubility, immunoreactivity and structure of major allergens in egg. *Food and Agricultural Immunology, 29*(1), 412–423.

Zhang, Z., Li, Y., Lee, M. C., Ravanfar, R., Padilla-Zakour, O. I., & Abbaspourrad, A. (2020). The impact of high-pressure processing on the structure and sensory properties of egg white-whey protein mixture at acidic conditions. *Food and Bioprocess Technology, 13*, 379–389.

Zhao, J., Li, Y., Xu, L., Zeng, J., Liu, Y., Timira, V., Zhang, Z., Lin, H., & Li, Z. (2022). Thermal induced the structural alterations, increased IgG/IgE binding capacity and reduced immunodetection recovery of tropomyosin from shrimp (*Litopenaeus vannamei*). *Food Chemistry, 391*, Article 133215.

Zhou, H., Wang, C., Ye, J., Chen, H., Tao, R., & Cao, F. (2016). Effects of high hydrostatic pressure treatment on structural, allergenicity, and functional properties of proteins from ginkgo seeds. *Innovative Food Science & Emerging Technologies, 34*, 187–195.

Zhu, Y., Vanga, S. K., Wang, J., & Raghavan, V. (2018). Impact of food processing on the structural and allergenic properties of egg white. *Trends in Food Science & Technology, 78*, 188–196.